Winding Losses in Coreless Axial Flux PM Machines with Wave and Spiral PCB Stator Topologies

Yaser Chulaee SPARK Lab, ECE Dept. University of Kentucky Lexington, KY, USA yaser.chulaee@uky.edu Donovin Lewis SPARK Lab, ECE Dept. University of Kentucky Lexington, KY, USA donovin.lewis@uky.edu Greg Heins
Regal Rexnord Corp.
Research and Development
Rowville, VIC, Australia
greg.heins@ieee.org

Dean Patterson Regal Rexnord Corp. Research and Development Rowville, VIC, Australia dean.patterson@ieee.org Dan M. Ionel
SPARK Lab, ECE Dept.
University of Kentucky
Lexington, KY, USA
dan.ionel@ieee.org

Abstract-Printed circuit board (PCB) stators in coreless axial flux permanent magnet (AFPM) machines have been proposed, designed and studied for utilization in multiple industries due to their design flexibility and reduction of manufacturing costs, volume, and weight compared to conventional stators. This paper investigated loss mechanisms and multiple methods of approximating winding supplementary losses in PCB stators with example wave and spiral winding topologies for a dual rotor, single stator configuration using 3D FEA models with a 15 hour runtime. The effect of rotor magnet placement, end windings, and active conductor path on eddy current is studied for both topologies. A hybrid FEA/analytical approach is proposed for the approximation of circulating current within layers of a planar PCB conductor using the equivalent circuit model. A coreless AFPM motor prototype is created and its power losses tested using multiple PCB stators with the findings being comparable to hybrid analytical methods results.

Index Terms—Axial-flux, coreless machines, FEA, permanent-magnet machines, PCB stator, winding losses, eddy current, circulating current.

I. INTRODUCTION

Axial flux permanent magnet synchronous machines (AF-PMSM) have faced an uptake in development in recent years for the removal of core-related losses and applications including electric vehicles (EV), heating, ventilation, and air conditioning (HVAC) systems, and industrial motor drives, etc. By removing the magnetic core, coreless type machines eliminate associated core losses to increase system efficiency. A critical component of coreless AFPM machines is the stator winding as, since the core loss has been eliminated, they are the main source of AC losses within the machine.

The introduction of printed circuit board (PCB) stators in AFPMSM has become a trending topic due to their reduced weight and volume, ease of accurate manufacturability, and allowing for more accessible mass production. The large flexibility in PCB stator coil shape, interconnection, and implementation has led to a multitude of studies focusing on their design and optimization for maximal efficiency [1–6]. Calculation of AC losses in PCB stators is essential towards winding design optimization prior to motor production as it contains the majority of component losses [4]. In [7], the authors derived a closed-form expression for eddy current losses within AFPM PCB stators which showed how important the width of the active conductor is, especially for high-speed AFPMSM [4, 8]. Within [9], eddy current losses in the brushless motor's PCB stator have been measured using a numerical method with a single magnetostatic solution and reasonable assumptions. For rotor imbalances that result in circulating currents and power loss, the authors of [4] developed a relationship showing how connection between layers directly contributes to power losses. Since each path is made up of a series of turns that are distributed across many layers, their corresponding back-emf depends on where the individual traces are located. Similarly in [5], it was proposed that rotor flux linkage between layer conductors are not the same, resulting in induced voltage differences between layers and circulating currents. As the number of layers increases, the difference in induced voltages increases, intensifying circulating currents [5]. Therefore, the selection of the number of layers, conductor paths, and their connected arrangement is essential.

Derived from previous studies describing wave [2, 10] and spiral winding topologies [3, 4], two PCB stators were designed, simulated in ANSYS Electronics, manufactured, and experimentally tested to approximate stator winding supplementary losses. This paper focuses on winding supplementary losses, i.e., eddy current and circulating current losses, that are very important for PCB stator integration and will be

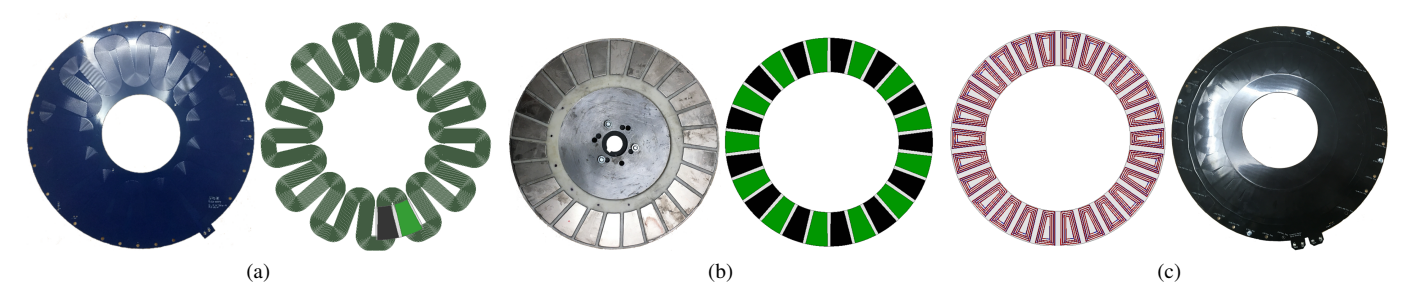


Fig. 1. PCB stator simulation models and motor hardware components for the wave winding stator (a), dual 26 pole rotor (b), and the spiral winding stator (c) used for ANSYS Maxwell simulation and the experimental motor prototype.

addressed in the following sections. The eddy and circulating current loss mechanisms were studied and numerically derived through 3D FEA and analytical methods considering the impacts of rotor and coil geometry, parallel and series connections and system sensitivity to rotor asymmetry. Experimentally, spin-down tests were performed for the derivation of PCB stator related power losses considering a loss separation technique.

II. PCB STATOR TOPOLOGIES

Studied PCB stators are comprised of planar copper conductor traces distributed axially on multiple layers through plated copper through-hole vias and radially with insulation between. Due to the planar nature of these traces, connections layer to layer and radially along the PCB stator require shape alteration to connect turns and coils as maximum torque is produced by maximizing radial trace alignment.

One of the major limitations in PCB stators is current carrying-capability of the conductor traces for field generation. Connecting planes of conductors in parallel or increasing conductor cross-sectional area are two measures to address this issue with a trade-off between Joule loss and eddy current loss minimization. For instance, stator eddy current losses are greatly reduced compared to conventional coreless AFPM machines due to the very small conductor cross-sectional area [4]. Current capability, however, is decreased with conductor area reduction and leads to parallel connections between traces to mitigate Joule losses in single conductors. Introduction of parallel paths for multi-layer connections increases the likelihood of circulating current generation between traces of different induced voltages within PCB layers, causing rotor imbalances [5]. These factors have led to many alternative approaches and designs for winding coil shapes and interconnections in previous works and industry [11], all of which boast varying electromagnetic properties greatly impacting machine performance.

The wave-type PCB stator winding, shown in Fig. 1(a), based on the topology explored in [10, 12] and optimized considering eddy losses in prior work [2], comprises 12 layers, 10 which contain active copper traces and two that are used as a path to route the return. On each active layer, there are 42 traces with a 0.14mm trace thickness, T_t , 0.2mm trace width and 0.25mm isolation width, grouped in six planar parallel

TABLE I SPECIFICATIONS OF SINGLE PHASE PCB STATOR WINDINGS WITH A $0.2 \mathrm{mm}$ Trace Width.

Winding type	Layer connection	N_t	N_L	T_t [mm]	OD [mm]	ID [mm]
Wave	Parallel	182	12	0.14	304.9	144.5
Spiral	Series	162	6	0.07	270.4	182.1

traces aggregated in series to form seven turns, a pattern which is repeated for all active layers, as summarized in Fig. 4. The equivalent number of turns per phase, N_t , is detailed in Table I for the wave winding from the product of the number of turns in one layer, seven, and the number of poles, 26. Vias are used to connect layers in parallel to increase current-carrying capability and apply system-balancing forces when facing rotor imbalances. The wave winding configuration maximizes active radial length, can host many pole pairs, and allows for easy layer stacking, however the turns are constrained by the outer and inner radii and manufacturing precision [10].

The spiral-type PCB stator winding, depicted in Fig. 1(c) described previously in [3, 4, 13], comprises six layers, all of which are active with a two layer coil pattern that radially connects the input and output terminals. On each active layer, there are 26 coils and each coil has 27 turns with an altered 0.07mm trace thickness with other system parameters summarized in Table I. Both configurations use a 26 pole rotor, shown in 1(b) on both sides to complete the flux path through the stator. Vias are used to connect all traces in series within one coil between layers and radially connect coils around the circumference via input/return bus bars. The spiral configuration maximizes coil area utilization, allows for a greater number of turns, and maximizes the torque to copper ratio, however it generates noncontributing torque due to angle relative to the motor center, and the active length is significantly shorter for inner tracks/turns [7]. FE models and physical prototypes of both PCB stators and the 26 pole double sided rotor are presented in Fig. 1.

III. WINDING LOSS MECHANISMS

One of the most critical factors in coreless electric machine design is avoiding or reducing eddy current losses in stator windings. Without the protection of slots, windings in coreless

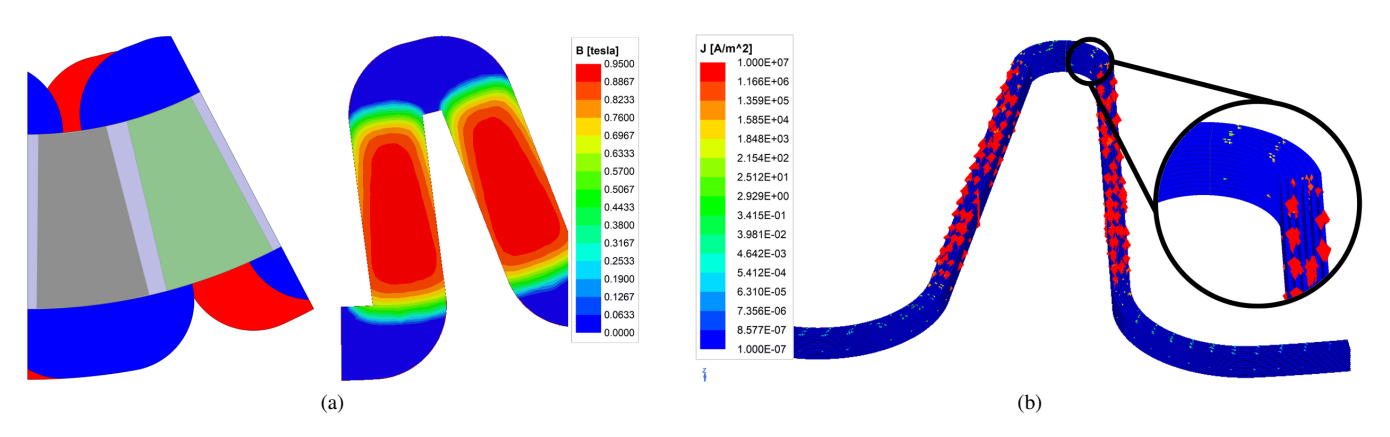


Fig. 2. Wave winding stator single pole pair 3D FE model and flux density distribution (a) and a diagram of the eddy current path in one turn (b). Since the dual rotor's magnets do not cover the coil's end windings, eddy current path is limited to the radial portion, shown in the detailed view.

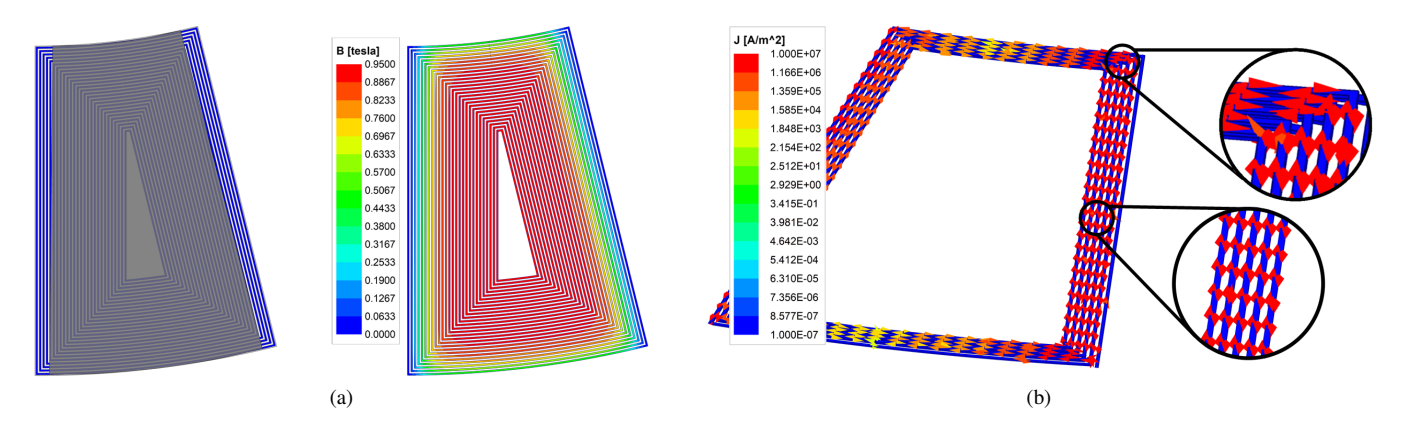


Fig. 3. Spiral winding stator single pole 3D FE model and flux density distribution (a) and a diagram of the eddy current path within 5 turns and 1 layers (b). Since the dual rotor's magnets cover the entire coil, eddy current path is not limited to the radial portion, propagating through the coil and from one layer to another.

AFPM machines are directly exposed to airgap flux density variations, causing eddy current within the stator's planar conductors, generating heat and non-contributing electromagnetic force[14]. Power dissipation of these eddy currents are dependent on the wire dimensions, material constants, and the operating frequency. For a PCB stator consisting of traces with a rectangular cross section, eddy current losses can be calculated [15]

$$P_{eddy} = \frac{\pi^2 N_c N_t f^2 t_w t_h l_m}{6\rho} \left(t_w^2 B_z^2 + t_h^2 B_\phi^2 \right) \tag{1}$$

where N_c is number of coil sides with average length of l_m , and N_t turns per coil. B_z and B_ϕ are axial and tangential components of the flux density, respectively. This equation also shows how PCB trace geometry affects eddy current losses. Where t_w is trace width and and t_h is trace height, in the z direction, and f denotes the frequency of flux variations.

The wave winding PCB stator, previously simulated and experimentally tested in [2], experiences eddy current losses caused by the shifting magnetic flux as indicated in Fig. 2(a). From the initial designs, copper trace dimension minimization and parallel paths were the focus for eddy current loss reduction [2]. The eddy current path, shown in Fig. 2(b),

is constrained to the radial conductor, preventing circulation through the system through the end winding as there is no flux nor current density. The 4.43mm copper trace skin depth is much larger than the conductor cross section of 0.2mm by 0.14mm with a 216Hz frequency at 1000rpm, greatly reducing eddy current power losses.

The flux density mapping of the spiral winding in Fig. 3(a) highlights that the rotor magnets fully cover the end winding during operation to utilize maximal active conductor but also extending a full eddy current path through a coil. Since there are more conductors covered by the rotor magnets at any point in time, there is more resistive heating and eddy current flows easily through the system. Vias within the center of the coils are used for traveling between layers and coil sections, allowing eddy current to generate and move between layers within the varying flux density region, as shown in Fig. 3(b). The detailed view shows how eddy current travels back and forth within the traces, similar to that of the wave winding with the derived eddy current loss reported in Table II.

Circulating currents within the stator winding is caused primarily by voltage differences between parallel paths. Equation (2) is a general expression for the calculation of circulating current losses within n parallel path with the equal resistance

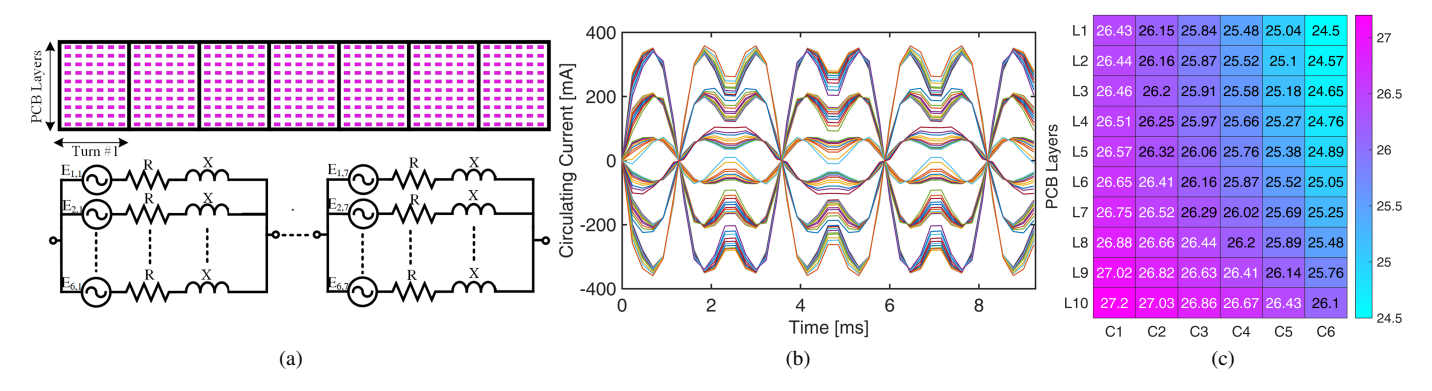


Fig. 4. Wave winding PCB stator diagrams including the conductor cross section for one phase and equivalent circuit for one layer (a), the open-circuit circulating currents in parallel traces within one turn (b), and a heat-map of the calculated induced voltages between copper traces within one turn over ten layers (c).

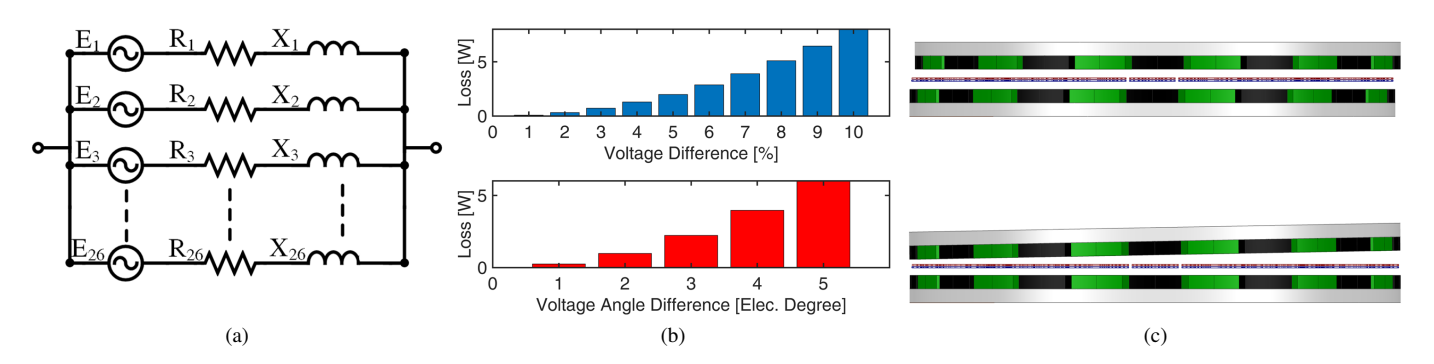


Fig. 5. Spiral winding PCB stator equivalent circuit diagram (a). Parametric studies for misalignment and rotor magnet properties for circulating current losses with varying voltage difference and voltage angle (b) and misalignment of the rotor (c) resulting in an approximate circulating current loss.

of R where the induced voltage of i^{th} path is denoted by E_i .

$$P_{circ.} = \sum_{i=1}^{n} RI_i^2 = \frac{1}{R} \sum_{i=1}^{n} \left[E_i - \frac{\sum_{i=1}^{n} E_i}{n} \right]^2$$
 (2)

Any rotor asymmetry in magnetic and geometric parameters can induce circulating currents within both PCB stators, of which the spiral design has much greater sensitivity. Parallel layers paths were used with typical manufacturing dimensions in our wave winding PCB design to test our proposed system of analysis for circulating current losses. Parallel paths reduce the conductor minimum size limitations due to Joule losses, approximated as resistances times current squared, while also creating a balancing magnetic force when imbalanced rotors are applied within the AFPM machine.

The circulating current power loss of the wave winding design can be approximated analytically using (2) based on the stator equivalent circuit shown in Fig. 4(a). Considering the 3D FEA results for rms circulating current in each trace, shown in Fig. 4(b), and the resistance of each trace, as a function of length, resistivity, and cross-sectional area, the calculated total circulating current power loss in all 420 traces is 28.3 W, as reported in Table II. The difference in induced voltages between conductors is depicted in Fig. 4(c)'s heat map with the x-axis split into six planar parallel traces per turn and the y-

axis representing ten active layers. Even with a perfect rotor, circulating current loss in the wave winding would still be present, originating from varying relative distances of parallel traces to the rotor magnets.

Focusing on parallel coils in the spiral winding as depicted in Fig. 5(a), the stator experiences greater sensitivity to rotor asymmetry which is often caused by manufacturing/installation errors, bearing wear, etc. Parametric equivalent circuit analysis based on variations in rotor parameters is employed to approximate circulating current power losses. Losses increased when the induced voltage angle difference between coils increased due to magnet displacement in the rotor, and also as the voltage amplitude difference increased due to uneven airgap and variation in individual magnet remanence, both shown in Fig. 5(b) and (c) respectively. Through this parametric study, it was found that a combination of amplitude and voltage angle difference originating from rotor asymmetry causes an approximate 10W power loss in the spiral winding PCB stator, reported in Table II in parenthesis.

IV. SIMULATION AND EXPERIMENTAL RESULTS

Having designed, analyzed, and simulated the two PCB stator designs, an experimental AFPM synchronous motor prototype was created as shown in Fig. 6(a). Spin down tests

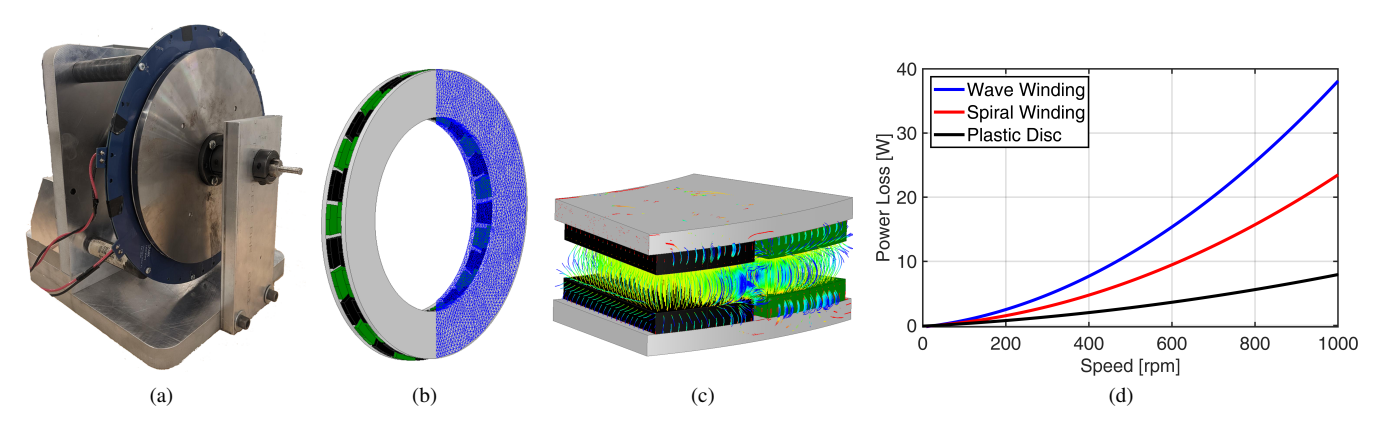


Fig. 6. Prototype single stator, dual rotor coreless AFPM machine (a), 3D FE model and mesh for the prototype machine with 15 hour runtime (b), airgap flux lines (c), and the experimental results derived from spin down tests for one phase operation (d).

TABLE II

SINGLE PHASE AC SUPPLEMENTARY COPPER LOSS EXPERIMENTAL
RESULTS AND FEA-BASED CIRCULATING AND EDDY CURRENT
COMPONENTS FOR OPEN-CIRCUIT OPERATING CONDITIONS AT 1,000
RPM.

Winding type	Experimental [W]	Circulating current [W]	Eddy current [W]
Wave	30.2	28.3	0.5
Spiral	15.6	(≈10)	1.1

were performed with rotor speed spun externally to a steady 1000rpm at which point the prime mover was decoupled and motor deceleration was measured with each PCB stator type. A plastic disc the same diameter as the PCB stator, similar to a process performed in [4, 16], was used to separate mechanical and electromagnetic loss components. The resulting power loss from all 3 cases is shown in Fig. 6(d).

Resulting losses from the experimental and FEA/analytical approximation methods are shown in Table II with the experimental losses matching the sum of circulating and eddy losses predicted. Circulating current losses within these designs were estimated to consist of majority of the losses present in the system. Computational and experimental analysis of circulating current losses, using the models shown in Fig.6(b) and (c), indicate that series connections should be made within PCB stator windings wherever possible to minimize current flowing between conductors of different induced voltages.

V. CONCLUSION

This paper investigated loss mechanisms for coreless AFPM synchronous machines integrating PCB stators with wave and spiral winding designs. For the studied windings, power loss components were individually approximated based on detailed 3D FE models and analytical methods.

Eddy current path limitations were studied to reduce eddy current loss in future PCB stator optimization and designs. Circulating current loss estimation methods have been developed to approximate power loss in varying planar conductors.

Furthermore, rotor asymmetry was found to contribute to losses and estimated using parametric equivalent circuit analysis. Open-circuit spin down tests were used to experimentally assess PCB stators' power losses, and the results were found to be comparable to FE-based analytical methods.

Within this study, it was found that optimization of coil geometry can reduce eddy losses significantly, however, parallel layers, used to improve current carrying capability and Joule losses, can greatly increase circulating currents and associated losses. Accurate methods of both eddy and circulating current loss approximation are essential to minimize AC supplementary copper losses.

ACKNOWLEDGMENT

This paper is based upon work supported by the National Science Foundation (NSF) under Award No. #1809876. Any opinions, findings, and conclusions, or recommendations expressed in this material are those of the authors and do not necessarily reflect the views of the NSF. The support of University of Kentucky, the L. Stanley Pigman Endowment, ANSYS Inc., and Regal Rexnord Corp. is also gratefully acknowledged.

REFERENCES

- O. Taqavi and S. M. Mirimani, "Design aspects, winding arrangements and applications of printed circuit board motors: a comprehensive review," *IET Electric Power Applications*, vol. 14, pp. 1505–1518, 2020.
- [2] P. Han, D. Lawhorn, Y. Chulaee, D. Lewis, G. Heins, and D. M. Ionel, "Design optimization and experimental study of coreless axial-flux pm machines with wave winding pcb stators," in 2021 IEEE Energy Conversion Congress and Exposition (ECCE), 2021, pp. 4347–4352.
- [3] D. Lawhorn, P. Han, D. Lewis, Y. Chulaee, and D. M. Ionel, "On the design of coreless permanent magnet machines for electric aircraft propulsion," in 2021 IEEE Transportation Electrification Conference Expo (ITEC), 2021, pp. 278–283.
- [4] F. Marcolini, G. De Donato, F. G. Capponi, and F. Caricchi, "Design of a high speed printed circuit board coreless axial flux permanent magnet machine," in 2021 IEEE Energy Conversion Congress and Exposition (ECCE), 2021, pp. 4353–4360.
- [5] N. S., S. P. Nikam, S. Singh, S. Pal, A. K. Wankhede, and B. G. Fernandes, "High-speed coreless axial-flux permanent-magnet motor

- with printed circuit board winding," *IEEE Transactions on Industry Applications*, vol. 55, no. 2, pp. 1954–1962, 2019.
- [6] H. Changchuang, B. Kou, X. Zhao, X. Niu, and L. Zhang, "Multi-objective optimization design of a stator coreless multidisc axial flux permanent magnet motor," *Energies*, vol. 15, p. 4810, 06 2022.
- [7] X. Wang, T. Li, P. Gao, and X. Zhao, "Design and loss analysis of axial flux permanent magnet synchronous motor with pcb distributed winding," in 2021 24th International Conference on Electrical Machines and Systems (ICEMS), 2021, pp. 1112–1117.
- [8] G. Francois and B. Dehez, "Impact of slit configuration on eddy current and supply current losses in pcb winding of slotless pm machines," *IEEE Transactions on Industry Applications*, pp. 1–1, 2022.
- [9] A. Ahfock and D. M. Gambetta, "Stator eddy-current losses in printed circuit brushless motors," *Iet Electric Power Applications*, vol. 5, pp. 159–167, 2011.
- [10] F. Marignetti, G. Volpe, S. M. Mirimani, and C. Cecati, "Electromagnetic design and modeling of a two-phase axial-flux printed circuit board motor," *IEEE Transactions on Industrial Electronics*, vol. 65, no. 1, pp. 67–76, 2018.
- [11] B. Anvari, P. Guedes-Pinto, and R. Lee, "Dual rotor axial flux permanent magnet motor using pcb stator," in 2021 IEEE International Electric Machines Drives Conference (IEMDC), 2021, pp. 1–7.

- [12] S. Paul, M. Farshadnia, A. Pouramin, J. Fletcher, and J. Chang, "A comparative analysis of wave winding topologies and performance characteristics in ultra-thin printed circuit board axial-flux permanent magnet machine," *IET Electric Power Applications*, 03 2019.
- [13] F. Tokgöz, G. Çakal, and O. Keysan, "Design and implementation of an optimized printed circuit board axial-flux permanent magnet machine," in 2020 International Conference on Electrical Machines (ICEM), vol. 1, 2020, pp. 111–116.
- [14] R. Wang and A. Kamper, "Evaluation of eddy current losses in axial flux permanent magnet (afpm) machine with an ironless stator," in Conference Record of the 2002 IEEE Industry Applications Conference. 37th IAS Annual Meeting (Cat. No.02CH37344), vol. 2, 2002, pp. 1289– 1294 vol.2.
- [15] N. Taran, D. M. Ionel, V. Rallabandi, G. Heins, and D. Patterson, "An overview of methods and a new three-dimensional fea and analytical hybrid technique for calculating ac winding losses in pm machines," *IEEE Transactions on Industry Applications*, vol. 57, no. 1, pp. 352–362, 2021.
- [16] G. Heins, D. Ionel, D. Patterson, S. Stretz, and M. Thiele, "Combined experimental and numerical method for loss separation in permanent magnet brushless machines," *IEEE Transactions on Industry Applica*tions, vol. 52, pp. 1–1, 01 2015.